Rydberg Electrons in a Bose-Einstein Condensate

Jia Wang, Marko Gacesa, and R. Côté
Department of Physics, University of Connecticut, Storrs, Connecticut 06269, USA
(Received 4 November 2014; revised manuscript received 27 March 2015; published 18 June 2015)

We investigate a hybrid system composed of ultracold Rydberg atoms immersed in an atomic Bose-Einstein condensate (BEC). The coupling between Rydberg electrons and BEC atoms leads to excitations of phonons, the exchange of which induces a Yukawa interaction between Rydberg atoms. Because of the small electron mass, the effective charge associated with this quasiparticle-mediated interaction can be large. Its range, equal to the BEC healing length, is tunable using Feshbach resonances to adjust the scattering length between BEC atoms. We find that for small healing lengths, the distortion of the BEC can "image" the Rydberg electron wave function, while for large healing lengths the induced attractive Yukawa potentials between Rydberg atoms are strong enough to bind them.

DOI: 10.1103/PhysRevLett.114.243003 PACS numbers: 32.80.Rm, 03.75.Hh, 63.20.kp

Impurities in a Bose-Einstein condensate (BEC) have motivated the investigation of a wide range of phenomena. For example, a single impurity can probe superfluidity [1–3], while an ionic impurity can form a mesoscopic molecular ion [4]. Because of the self-energy induced by phonons (BEC excitations), a neutral impurity can self-localize in BECs [5–7], shedding light on polaron physics [8,9]. Phonon exchange induces an attractive Yukawa potential between impurities [10,11], leading to the so-called "co-self-localization" [12] and the formation of bi- and multipolarons [13]. Recent experiments, where a BEC atom is excited into a Rydberg state [14], open the door to explorations of the electron-phonon coupling in ultracold degenerate gases, a phenomenon reminiscent of the formation of Cooper pairs of repelling electrons in superconductivity [15].

In this Letter, we study Rydberg atoms immersed in a homogeneous BEC [Fig. 1(a)]. Rydberg atoms consist of an ion core and a highly excited electron with its oscillatory wave function Ψ_e extending to large distances of the order of $\sim n^2 a_0$ (n is the principle quantum number and a_0 the Bohr radius). In contrast to "traditional" neutral impurities in a BEC [10–13], the interaction between Rydberg and BEC atoms is dominated by the electron-atom interaction, which allows stronger impurity–BEC-atom coupling and independent control of interaction between BEC atoms with Feshbach resonances. In addition, the large extent of Ψ_e makes it possible to "imprint" the electronic wave function on BEC density modulations.

As pointed out by Fermi [16], the interaction between the quasifree electron at $\mathbf{x}$ and a ground state atom at $\mathbf{r}$ can be approximated at low scattering energies by a contact interaction parametrized by an energy-dependent s-wave scattering length $A_s(k) = -k^{-1} \tan \delta_s(k)$

$$V_s(\mathbf{x}, \mathbf{r}) = \frac{2\pi\hbar^2}{m_e} A_s\big(k(r)\big)\delta^{(3)}(\mathbf{x} - \mathbf{r}). \tag{1}$$

While the s-wave approximation is useful for qualitative analysis, we include higher-partial wave contributions for quantitative results [17]. The local wave number $k(r)$ is

$$\frac{\hbar^2 k(r)^2}{2m_e} = -\frac{\mathcal{R}_y}{(n-\delta_{\ell_e})^2} + \frac{e^2}{4\pi\epsilon_0 r}, \tag{2}$$

where $\mathcal{R}_y$ is the Rydberg constant, ϵ_0 is the vacuum permittivity, and e and m_e are the charge and mass, respectively, of the electron with angular momentum ℓ_e and quantum defect δ_{ℓ_e}. For low-ℓ_e states, Eq. (1) gives an effective interaction between Rydberg and ground state atoms as

$$V_R(\mathbf{r}) \approx \frac{2\pi\hbar^2 A_s[k(r)]}{m_e} |\Psi_e(\mathbf{r})|^2, \tag{3}$$

(a)

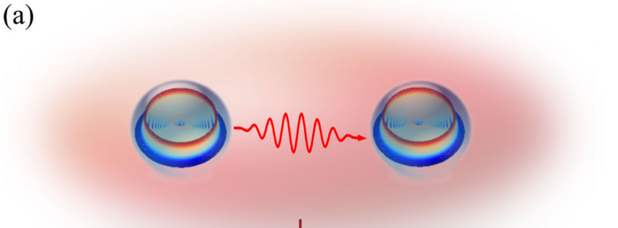

(b)

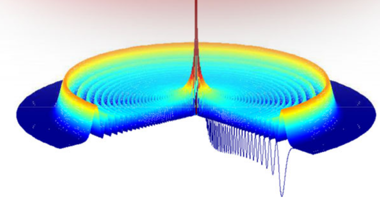

FIG. 1 (color online). (a) Sketch: two Rydberg atoms immersed in a BEC exchange phonons. $|\Psi_e|^2$ is represented by the surface inside each sphere. (b) $|\Psi_e|^2$ along with the interaction potential curve within the s-wave approximation.

which leads to an attraction and formation of ultra-long-range Rydberg molecules for $A_s < 0$ [18]. The electron density and corresponding oscillatory potential are sketched in Fig. 1(b) for a Rydberg ns ($\ell_e = 0$) state. High-ℓ_e states with negligible δ_{ℓ_e} are nearly degenerate, and their coupling gives electronic wave functions with complex quantum interference patterns. For alkali metals (e.g., Rb or Cs), these interactions can support very extended bound "trilobite states" that possess a strong permanent dipole moment. The observation of trilobitelike states [19–23] has motivated the studies of the p-wave electron (leading to "butterfly states" [24]) and Rydberg electrons scattering off a perturber with a permanent dipole moment [25].

Here, Rydberg electrons interact with the many-atom BEC, resulting in collective excitations (phonons). The phonon exchange in a BEC leads to a Yukawa potential. We find two regimes based on the BEC healing length ξ. For small ξ, the Yukawa potential is short ranged and distorts the BEC locally, "mapping" $|\Psi_e|^2$ onto the BEC density. For large ξ, the Yukawa potential is long ranged and can bind Rydberg atoms together.

We first consider a homogeneous BEC in the absence of impurities, described by the Hamiltonian

$$H_{\mathrm{BEC}} = \sum_{\mathbf{k}} \frac{\hbar^2 k^2}{2m_B} c_{\mathbf{k}}^\dagger c_{\mathbf{k}} + \frac{u_B}{2\Omega_V} \sum_{kpq} c_{\mathbf{k}}^\dagger c_{\mathbf{p}}^\dagger c_{\mathbf{q}} c_{\mathbf{k}+\mathbf{p}-\mathbf{q}}, \quad (4)$$

where $u_B = 4\pi\hbar^2 a_B/m_B$ is the coupling between the atoms of mass m_B and scattering length a_B, Ω_V is the quantization volume, and $c_{\mathbf{k}}^\dagger$ ($c_{\mathbf{k}}$) is the creation (annihilation) operator of bosonic atoms with momentum $\mathbf{k}$. If most atoms occupy the ground state ($\mathbf{k} = \mathbf{0}$), one can replace $c_0^\dagger$ and c_0 by $\sqrt{N_0}$ and expand Eq. (4) in decreasing order of N_0. The number of atoms is given by $N = N_0 + \sum_{\mathbf{k}\neq\mathbf{0}} c_{\mathbf{k}}^\dagger c_{\mathbf{k}}$. By keeping terms of the order of $\sqrt{N_0}$ or higher, H_{BEC} can be diagonalized via the Bogoliubov transformation $c_{\mathbf{q}}^\dagger = u_q b_{\mathbf{q}}^\dagger + v_q b_{-\mathbf{q}}$. The resulting effective Hamiltonian is $\mathcal{H}_{\mathrm{BEC}} = \sum_{\mathbf{q}} \hbar\omega_q (b_{\mathbf{q}}^\dagger b_{\mathbf{q}} + 1/2)$, where $\hbar\omega_q = (\epsilon_q^2 + 2u_B\rho_B\epsilon_q)^{1/2}$, with $\epsilon_q = \hbar^2 q^2/2m_B$ and the BEC number density $\rho_B = N/\Omega_V$. The Bogoliubov operator $b_{\mathbf{q}}^\dagger$ ($b_{\mathbf{q}}$) creates (annihilates) a quasiparticle (or phonon) of momentum $\mathbf{q}$ when applied to the ground state $|0\rangle$: $b_{\mathbf{q}}^\dagger|0\rangle = |\mathbf{q}\rangle$. The local density operator $\hat{\rho}(\mathbf{r}) = \Omega_V^{-1}\sum_{\mathbf{p},\mathbf{q}} e^{i\mathbf{q}\cdot\mathbf{r}} c_{\mathbf{p}+\mathbf{q}}^\dagger c_{\mathbf{p}}$ becomes

$$\hat{\rho}(\mathbf{r}) \approx \frac{N_0}{\Omega_V} + \frac{\sqrt{N_0}}{\Omega_V} \sum_{\mathbf{q}\neq 0} e^{i\mathbf{q}\cdot\mathbf{r}} (u_{\mathbf{q}} + v_{\mathbf{q}})(b_{\mathbf{q}}^\dagger + b_{-\mathbf{q}}) \quad (5)$$

and the interaction between a Rydberg electron and BEC atoms $H_{\mathrm{int}} = \int d^3 r \rho(\mathbf{r}) V_R(\mathbf{r})$ is

$$H_{\mathrm{int}} \approx \frac{N_0}{\Omega_V} V_0 + \frac{\sqrt{N_0}}{\Omega_V} \sum_{\mathbf{q}\neq 0} (u_{\mathbf{q}} + v_{\mathbf{q}})(b_{\mathbf{q}}^\dagger + b_{-\mathbf{q}}) V_{\mathbf{q}}, \quad (6)$$

where $V_{\mathbf{q}} = \int d^3 r V_R(\mathbf{r}) e^{i\mathbf{q}\cdot\mathbf{r}}$ is the Fourier transform of $V_R(\mathbf{r})$ in Eq. (3). The first and second order corrections to the ground state energy are $E^{(1)} = \int d^3 r \rho_B V_R(\mathbf{r})$ and

$$E^{(2)} = -\frac{m_B}{2\pi\hbar^2} \int d^3 r d^3 r' \rho_B V_R(\mathbf{r}) \frac{e^{-|\mathbf{r}-\mathbf{r}'|/\xi}}{|\mathbf{r}-\mathbf{r}'|} V_R(r'), \quad (7)$$

where we take the thermodynamic limit of $\Omega_V^{-1}\sum_{\mathbf{q}} \to (2\pi)^{-3} \int d^3 q$ and integrate over $\mathbf{q}$. At this level of approximation, N_0 can be replaced by N.

Using $V_R(\mathbf{r})$ from Eq. (3), and assuming ρ_B constant (homogeneous BEC), $E^{(1)} = 2\pi\rho_B\hbar^2\bar{a}_e/m_e$ is the mean-field energy shift, where $\bar{a}_e = \int d^3 r A_s[k(r)]|\Psi_e(\mathbf{r})|^2$ is an average scattering length [26], while $E^{(2)} \approx \int d^3 r d^3 r' |\Psi_e(\mathbf{r})|^2 V_Y(\mathbf{r}-\mathbf{r}')|\Psi_e(\mathbf{r}')|^2/2$ involves the Yukawa potential

$$V_Y(\mathbf{r}-\mathbf{r}') = -\tilde{Q}^2 \frac{e^{-|\mathbf{r}-\mathbf{r}'|/\xi}}{|\mathbf{r}-\mathbf{r}'|}, \quad (8)$$

where its range $\xi = 1/\sqrt{16\pi\rho_B a_B}$ equals the BEC healing length, and $\tilde{Q}^2 \approx 4\pi\hbar^2\bar{a}_e^2\rho_B m_B/m_e^2$ characterizes its strength [26]; the "effective charge" $\tilde{Q}$ emphasizes the analogy with Coulomb interactions. The term $E^{(2)}$ can be understood as the self-interaction of electrons by a Yukawa potential induced via phonon exchange at two different positions. This term is crucial in studies of self-localization of impurities in a BEC [10–13]. Here, the Rydberg electrons are already localized by strong Coulomb forces with ion cores. Therefore, the distorted BEC density, under appropriate conditions, can reflect the oscillatory nature of Ψ_e and "image" the Rydberg electron.

To first order, the perturbed ground state given by $|\tilde{0}\rangle = |0\rangle - (\sqrt{N_0}/\Omega_V)\sum_{\mathbf{q}\neq\mathbf{0}}(u_{\mathbf{q}} + v_{\mathbf{q}})V_{\mathbf{q}}/(\hbar\omega_q)|\mathbf{q}\rangle$ leads to the BEC density distortion $\delta\rho(r) \equiv \langle\hat{\rho}(r)\rangle - \rho_B$

$$\delta\rho(\mathbf{r}) = -\frac{m_B\rho_B}{\hbar^2\pi} \int d^3 r' V_R(\mathbf{r}') \frac{e^{-|\mathbf{r}-\mathbf{r}'|/\xi}}{|\mathbf{r}-\mathbf{r}'|}. \quad (9)$$

Equation (9) shows that $\delta\rho(\mathbf{r})$ is affected by "averaging" V_R within the range ξ. The oscillatory nature of Ψ_e can be imaged onto $\delta\rho(\mathbf{r})$ [27]. However, if ξ is larger than the local wavelength of the Rydberg electron, the averaging will erase this signature. Figure 2(a) compares the radial probability density $P_e(x) = 4\pi x^2|\Psi_e(x)|^2$ with $\Delta P(r) = 4\pi r^2\delta\rho(r)$ for a ^{87}Rb(160s) Rydberg atom in a ^{87}Rb BEC with $\rho_B = 2\times 10^{13}$ cm^{-3} for different scattering lengths a_B. Larger values of a_B produce sharper oscillations, albeit overall smaller amplitudes. This is better illustrated by the "normalized" 2D distortion densities $\Delta P_{2\mathrm{D}}/\max(\Delta P_{2\mathrm{D}})$ in the xy plane in Fig. 2(b), where $\Delta P_{2\mathrm{D}} = 2\pi r\delta\rho$. Each quadrant corresponds to a different value of a_B, with portions enlarged in Fig. 2(c): the oscillations for $a_B = 20\times 10^3$ a.u. (quadrant A) are sharper than for

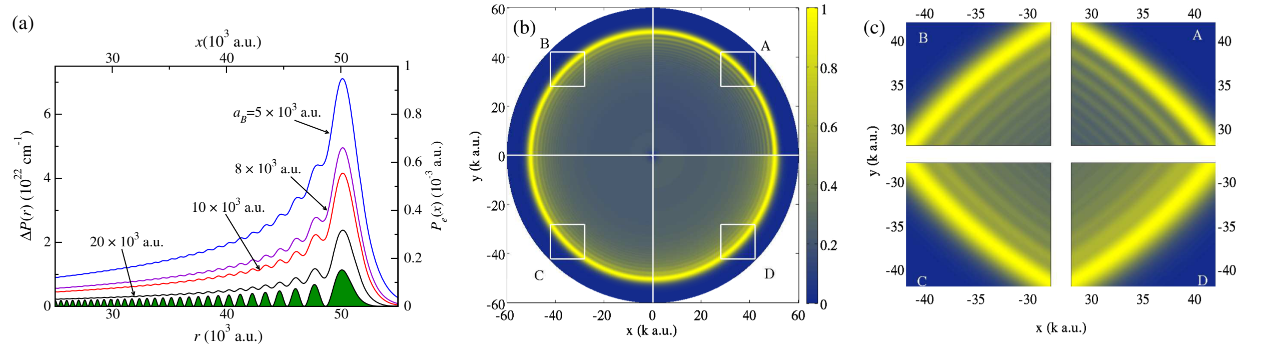

FIG. 2 (color online). (a) Comparison of $P_e(x) = 4\pi x^2|\Psi_e(x)|^2$ (green filled curve) and $\Delta P(r) = 4\pi r^2 \delta\rho(r)$ (solid curves) for a ^{87}Rb BEC at density $\rho_B = 2\times 10^{13}$ cm^{-3} for various scattering lengths a_B (in units of $k = 10^3 a_0$). (b) BEC density distortion $\Delta P_{2D}/\max(\Delta P_{2D})$, where $\Delta P_{2D} = 2\pi r\delta\rho$,with quadrant A, B, C and D correspondingto $a_B = 20\times 10^3, 10\times 10^3, 8\times 10^3$, and 5×10^3 a.u., respectively. (c) Enlargements of the regions are outlined in (b).

$a_B = 5\times 10^3$ a.u. (quadrant D), with amplitudes a few percent of the average BEC density. These show the possibility for *in situ* imaging of $|\Psi_e|^2$. We note that because the electron-Rb interaction is attractive, the Rydberg atoms will tend to migrate towards the largest BEC densities (the center of a trapped BEC), as opposed to the case of superfluid helium droplets, for which Rydberg atoms migrate to the surface due to a repulsive electron-He interaction. The Rydberg atoms' finite lifetime imposes additional experimental challenges; however, an upper limit $\tau_B = m_B\xi^2/\hbar$ for the BEC response time [12] (a few microseconds here) is much shorter than the radiative lifetime of Rydberg atoms [28].

For large healing lengths ξ, the averaging of V_R masks the electron self-interaction. However, phonon exchange still mediates nontrivial interactions between Rydberg atoms. Without a BEC, two Rydberg atoms experience strong long-range interactions, leading to formation of macrodimers [29] and the excitation blockade [30–34]. For two ns Rydberg atoms separated by R, it is repulsive with its leading contribution being the van der Waals (vdW) $+\,C_6/R^6$ term, where $C_6 \propto n^{11}$ [35]. Immersed in a BEC, however, the exchange of phonons between two Rydberg atoms gives rise to a Yukawa potential. We derive this potential within the Born-Oppenheimer (BO) approximation, starting from the interaction of two Rydberg atoms, located at $\mathbf{R}_1$ and $\mathbf{R}_2$, and BEC atoms (after applying the Bogoliubov transformation)

$$H_{\rm int} \approx \frac{N_0}{\Omega_V}({}^1\mathcal{V}_0 + {}^2\mathcal{V}_0) + \sum_{\mathbf{q}\neq\mathbf{0}}(u_q + v_q) \times (b^\dagger_{\mathbf{q}} + b_{-\mathbf{q}})({}^1\mathcal{V}_{\mathbf{q}}e^{i\mathbf{q}\cdot\mathbf{R}_1} + {}^2\mathcal{V}_{\mathbf{q}}e^{i\mathbf{q}\cdot\mathbf{R}_2}). \quad (10)$$

Here, ${}^i\mathcal{V}_{\mathbf{q}} \equiv \int d^3r V_i(\mathbf{r})e^{i\mathbf{q}\cdot\mathbf{r}}$, where $V_i(\mathbf{r})$ describes the interaction of "impurity" i with BEC atoms in coordinate space. Within perturbation theory, the first order correction $E^{(1)}$ gives a mean-field energy shift similar to the single Rydberg atom case in the thermodynamic limit. For spherically symmetric interactions (where ${}^i\mathcal{V}_{\mathbf{q}} = {}^i\mathcal{V}_{-q} = {}^i\mathcal{V}_q$ is real) and assuming ρ_B constant, the second order correction is

$$E^{(2)} = -\frac{\rho_B}{(2\pi)^3}\int d^3q \frac{A_q + 2B_q e^{iqR\cos\theta_q}}{\epsilon_q + 2u_B\rho_B}, \quad (11)$$

where $A_q = ({}^1\mathcal{V}_q)^2 + ({}^2\mathcal{V}_q)^2$, $B_q = {}^1\mathcal{V}_q \times {}^2\mathcal{V}_q$, $R = |\mathbf{R}_1 - \mathbf{R}_2|$, and θ_q is the angle between $\mathbf{R}$ and $\mathbf{q}$. The term containing A_q can be understood as the self-localizing energy for both Rydberg atoms calculated previously and contributes a constant energy shift. Together with the mean-field energy shift provided by $E^{(1)}$, these contributions can be omitted in the study of the relative dynamics of Rydberg atoms: only the term containing B_q gives an R-dependent energy shift leading to the BO potential

$$U(R) = -\frac{\rho_B}{(2\pi)^3}\int d^3q \frac{2B_q e^{iqR\cos\theta_q}}{\epsilon_q + 2u_B\rho_B}, \quad (12)$$

which can be easily generalized to interactions between any two impurities immersed in a BEC [11]. The $e^{iqR\cos\theta_q}$ term implies that only small q values contribute for large R, leading to the asymptotic behavior $U(R) \to -\tilde{Q}^2 e^{-R/\xi}/R$, where $\tilde{Q}^2 \approx \rho_B m_B B_{q=0}/\pi$. Within the s-wave approximation, the effective charge is $\tilde{Q}^2 \approx 4\pi\hbar^2\bar{a}_e^2\rho_B m_B/m_e^2$ as before. Not surprisingly, we obtain the same Yukawa potential as in Eq. (8), since phonon exchange mediates the interaction. Note that $\tilde{Q}$ is inversely proportional to m_e for Rydberg atoms since the electrons are really the perturbers, as opposed to more massive neutral impurities of mass m_I for which $\tilde{Q}$ is inversely proportional to m_I. Hence, the induced interaction is much stronger for Rydberg atoms.

The BO approach allows the study of corrections induced by the motion of Rydberg atoms (i.e., impurity atoms of mass m_I). The BO diagonal correction is $\Delta E^{(2)} = \hbar^2\langle\tilde{0}|\overleftarrow{\partial}_R\vec{\partial}_R|\tilde{0}\rangle/m_I$, where $|\tilde{0}\rangle = |0\rangle - \sum_{\mathbf{q}\neq\mathbf{0}}[(\langle\mathbf{q}|H_{\rm int}|0\rangle)/\hbar\omega_q]|\mathbf{q}\rangle$ is the perturbed ground state. Therefore, $\Delta E^{(2)} = (\hbar^2/m_I)\sum_{\mathbf{q}\neq\mathbf{0}}[(\langle 0|\partial_R H_{\rm int}|\mathbf{q}\rangle\times$

$\langle \mathbf{q}|\partial_R H_{\rm int}|0\rangle)/\hbar^2\omega_q^2]$, so that, in the thermodynamic limit and neglecting the constant energy shift terms, the BO diagonal correction to $U(R)$ is

$$\Delta U(R) = -\frac{\hbar^2}{2m_I}\frac{\rho_B}{(2\pi)^3}\int d^3q \frac{B_q q^2 \cos^2\theta_q e^{iqR\cos\theta_q}}{\sqrt{\epsilon_q(\epsilon_q + 2u\rho_B)^3}}. \quad (13)$$

As for $U(R)$, only small q values contribute for large R, so that $\Delta U(R) \to (m_B/m_I)(\tilde{Q}^2/2\xi)F(R/\xi)$, with $F(x)$ defined as $F(x) = (2/\pi) - (4/\pi x^2) - [2f(-1,x)/x^2] + [f(0,x)/x] - f(1,x)$, where $f(n,x) = I_n(x) - L_n(x)$ is given in terms of the modified Bessel function of the first kind $I_n(x)$ and the modified Struve function $L_n(x)$. The asymptotic behaviors are $F(R/\xi) \to 4/(3\pi)$ for $R \ll \xi$, and $F(R/\xi) \to 12\xi^4/(\pi R^4)$ for $R \gg \xi$. We note that for $R \gg \xi$, these imply a vanishing adiabatic potential $U(R)$ and a BO diagonal correction dominated by a repulsive $1/R^4$ term. As expected, ΔU can be neglected if $m_B \ll m_I$. Another limit is reached for a very large ξ, achievable using a Feshbach resonance to tune $a_B \to 0$. Then, the BO diagonal correction also vanishes: $\lim_{\xi\to\infty}\Delta U(R) = 0$, even when m_B is larger than m_I. In this limit, $U(R)$ does not vanish but reduces to the Coulomb potential $-\tilde{Q}^2/R$.

We illustrate these predictions with two ^{87}Rb(50s) Rydberg atoms immersed in a ^{87}Rb BEC with $\rho_B = 10^{13}$ cm^{-3}. To ensure a healing length ξ much larger than the Rydberg atoms, a_B is tuned to 10 a.u. (e.g., via a Feshbach resonance), so that $\xi = 3.66 \times 10^4$ a.u. The numerical "trilobitelike" interaction shown in Fig. 3(a) is constructed using the first-order perturbative model [16,36] including s and p contributions [17], with zero-energy scattering lengths $A_s(0) = -16.05a_0$ [37]. The states in the range $n = 21$–72 were included and the resulting Hamiltonian diagonalized to obtain the 50s eigenstate [38]. Figure 3(b) shows that B_q converges to a constant $B_{q=0} \approx 2 \times 10^4$ a.u. for a small q, yielding an effective charge $\tilde{Q}^2 \approx 1.54 \times 10^{-3}$ a.u. Figure 3(c) depicts the effect of immersing Rydberg atoms in a BEC: without the BEC, two Rydberg atoms interact via the vdW potential $C_6/R^6 + C_8/R^8 + C_{10}/R^{10}$ [repulsive solid-red curve in Fig. 3(b) with $C_6 = 1.074 \times 10^{20}$, $C_8 = -7.189 \times 10^{26}$, and $C_{10} = 7.162 \times 10^{33}$, in a.u. for ^{87}Rb(50$s$) [39].] In a BEC, the BO potential (solid black curve) is attractive at large separations, following the Yukawa potential $-\tilde{Q}^2 e^{-R/\xi}/R$ (dash-dotted curve), before becoming repulsive at shorter range where the "bare" repulsive vdW interaction dominates the phonon-exchange contribution. The resulting well can support bound levels; here, its depth is about -17.77 MHz and its equilibrium separation about 60×10^3 a.u. (much larger than the 5×10^3 a.u. extension of the trilobitelike potentials). The large mass of Rb leads to many bound levels; the three lowest are at about -17.64 MHz, -17.56 MHz, and -17.47 MHz. The ground state wave function with a spatial width of about

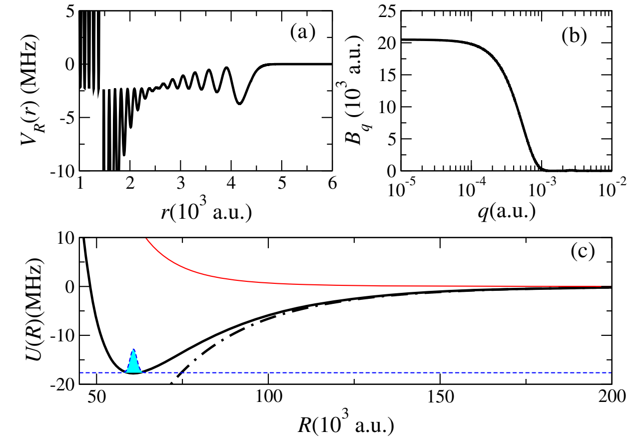

FIG. 3 (color online). (a) Potential between ^{87}Rb atoms in ground and 50s states. (b) B_q as a function of q. (c) Interaction between two Rydberg ^{87}Rb(50s) atoms in a BEC (solid black curve) and in vacuum (solid red curve). The Yukawa potential dominates the tail (dash-dotted curve) while the blue filled curve represents the lowest bound state.

2×10^3 a.u. is also shown in Fig. 3(c). The BO diagonal correction ΔU is less than 5% (+0.85 MHz near the well minimum) and decreases at larger R.

These results show how phonon exchange modifies an otherwise repulsive interaction into a potential well capable of binding two Rydberg atoms. Figure 4 explores its sensitivity to variations in ρ_B and a_B, and compares them to the bare case (without a BEC). The behavior of the BO curves can be understood qualitatively from the s-wave approximation. For a fixed a_B, the competition of $\tilde{Q}^2 \propto \rho_B$ and $\xi \propto \rho_B^{-1/2}$ leads to a deeper BO curve for a moderate density [see Fig. 4(a)]. However, $\tilde{Q}^2$ is independent of a_B while ξ is proportional to $a_B^{-1/2}$, giving deeper BO curves as a_B gets smaller [see Fig. 4(a)]. Hence, the BEC-induced interaction can be conveniently controlled by tuning a_B via

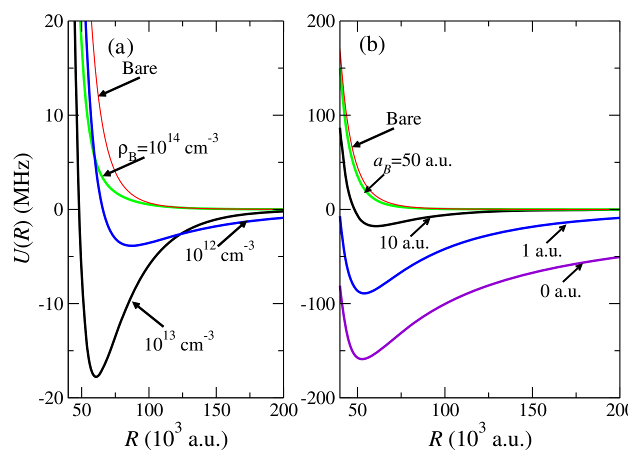

FIG. 4 (color online). Bare interaction (solid red line) and BO curves between two ^{87}Rb(50s) atoms for (a) different densities ρ_B and fixed $a_B = 10$ a.u. and for (b) different scattering lengths a_B and fixed $\rho_B = 10^{13}$ cm^{-3}.

a Feshbach resonance; in the limit $a_B \to 0$, the long-range Yukawa potential becomes an attractive Coulomb potential.

In summary, we studied the interaction between Rydberg atoms mediated by phonon exchange in an atomic BEC and found two limiting cases with respect to the BEC healing length ξ. For small ξ, the BEC density modulation can image the wave function of the Rydberg electron, while large ξ leads to attractive wells strong enough to bind Rydberg atoms. These wells are easily controlled by tuning a_B, e.g., to generate "synthetic" Coulomb potentials as $a_B \to 0$. Studies of Rydberg atoms immersed in BECs open promising avenues of research such as bi- and multipolaron physics [13] or co-self-localization [12], possible Rydberg crystallization [40], or the phase diagram of Yukawa bosons [41]. Finally, they offer the opportunity to investigate systems where electron-phonon coupling plays a crucial role under conditions different from the standard BCS physics.

This work was partially supported by the Grant No. DE-FG02-05ER15734 funded by the U.S. Department of Energy, Office of Science (J. W.), the Grant No. W911NF-13-1-0213 funded by the U.S. Army Research Office (M. G.), and the Grant No. PHY 1101254 funded by the National Science Foundation (R. C).

[1] E. Timmermans and R. Côté, Phys. Rev. Lett. **80**, 3419 (1998).
[2] A. P. Chikkatur, A. Görlitz, D. M. Stamper-Kurn, S. Inouye, S. Gupta, and W. Ketterle, Phys. Rev. Lett. **85**, 483 (2000).
[3] G. E. Astrakharchik and L. P. Pitaevskii, Phys. Rev. A **70**, 013608 (2004).
[4] R. Côté, V. Kharchenko, and M. D. Lukin, Phys. Rev. Lett. **89**, 093001 (2002).
[5] K. Sacha and E. Timmermans, Phys. Rev. A **73**, 063604 (2006).
[6] R. M. Kalas and D. Blume, Phys. Rev. A **73**, 043608 (2006).
[7] M. Bruderer, W. Bao, and D. Jaksch, Europhys. Lett. **82**, 30004 (2008).
[8] F. M. Cucchietti and E. Timmermans, Phys. Rev. Lett. **96**, 210401 (2006).
[9] A. A. Blinova, M. G. Boshier, and E. Timmermans, Phys. Rev. A **88**, 053610 (2013).
[10] L. Viverit, C. J. Pethick, and H. Smith, Phys. Rev. A **61**, 053605 (2000).
[11] M. J. Bijlsma, B. A. Heringa, and H. T. C. Stoof, Phys. Rev. A **61**, 053601 (2000).
[12] D. H. Santamore and E. Timmermans, New J. Phys. **13**, 103029 (2011).
[13] W. Casteels, J. Tempere, and J. T. Devreese, Phys. Rev. A **88**, 013613 (2013).
[14] J. B. Balewski, A. T. Krupp, A. Gaj, D. Peter, H. P. Büchler, R. Löw, S. Hofferberth, and T. Pfau, Nature (London) **502**, 664 (2013).
[15] J. Bardeen, L. N. Cooper, and J. R. Schrieffer, Phys. Rev. **108**, 1175 (1957).
[16] E. Fermi, Nuovo Cimento **11**, 157 (1934).
[17] $V_p(\mathbf{x},\mathbf{r}) = (6\pi\hbar^2/m_e)A_p^3(k)\delta^{(3)}(\mathbf{x}-\mathbf{r})\overleftarrow{\nabla}\cdot\vec{\nabla}$ for p waves, with $k^3A_p^3(k) = -\tan\delta_p(k)$.
[18] C. H. Greene, A. S. Dickinson, and H. R. Sadeghpour, Phys. Rev. Lett. **85**, 2458 (2000).
[19] V. Bendkowsky, B. Butscher, J. Nipper, J. P. Shaffer, R. Löw, and T. Pfau, Nature (London) **458**, 1005 (2009).
[20] W. Li, T. Pohl, J. M. Rost, S. T. Rittenhouse, H. R. Sadeghpour, J. Nipper, B. Butscher, J. B. Balewski, V. Bendkowsky, R. Löw *et al.*, Science **334**, 1110 (2011).
[21] M. A. Bellos, R. Carollo, J. Banerjee, E. E. Eyler, P. L. Gould, and W. C. Stwalley, Phys. Rev. Lett. **111**, 053001 (2013).
[22] A. Krupp, A. Gaj, J. Balewski, P. Ilzhöfer, S. Hofferberth, R. Löw, T. Pfau, M. Kurz, and P. Schmelcher, arXiv:1401.2477v1.
[23] D. A. Anderson, S. A. Miller, and G. Raithel, arXiv:1401.2477v1.
[24] E. L. Hamilton, C. H. Greene, and H. R. Sadeghpour, J. Phys. B **35**, L199 (2002).
[25] M. Mayle, S. T. Rittenhouse, P. Schmelcher, and H. R. Sadeghpour, Phys. Rev. A **85**, 052511 (2012).
[26] For high n Rydberg states, $A_s[k(r)] \simeq A_s(0)$, so that $\bar{a}_e \simeq A_s(0)\int d^3r|\Psi_e(\mathbf{r})|^2 = A_s(0)$.
[27] T. Karpiuk, M. Brewczyk, K. Rzażewski, J. B. Balewski, A. T. Krupp, A. Gaj, R. Löw, S. Hofferberth, and T. Pfau, arXiv:1402.6875.
[28] The origin of shorter lifetimes of a few tens of microseconds observed in a BEC [27] is under investigation. However, they are still an order of magnitude longer than τ_B.
[29] C. Boisseau, I. Simbotin, and R. Côté, Phys. Rev. Lett. **88**, 133004 (2002).
[30] M. D. Lukin, M. Fleischhauer, R. Cote, L. M. Duan, D. Jaksch, J. I. Cirac, and P. Zoller, Phys. Rev. Lett. **87**, 037901 (2001).
[31] D. Tong, S. M. Farooqi, J. Stanojevic, S. Krishnan, Y. P. Zhang, R. Côté, E. E. Eyler, and P. L. Gould, Phys. Rev. Lett. **93**, 063001 (2004).
[32] K. Singer, M. Reetz-Lamour, T. Amthor, L. G. Marcassa, and M. Weidemüller, Phys. Rev. Lett. **93**, 163001 (2004).
[33] T. Vogt, M. Viteau, J. Zhao, A. Chotia, D. Comparat, and P. Pillet, Phys. Rev. Lett. **97**, 083003 (2006).
[34] T. Cubel Liebisch, A. Reinhard, P. R. Berman, and G. Raithel, Phys. Rev. Lett. **95**, 253002 (2005).
[35] K. R. Overstreet, A. Schwettmann, J. Tallant, D. Booth, and J. P. Shaffer, Nat. Phys. **5**, 581 (2009).
[36] A. Omont, J. Phys. (Paris) **38**, 1343 (1977).
[37] V. Bendkowsky, B. Butscher, J. Nipper, J. B. Balewski, J. P. Shaffer, R. Löw, T. Pfau, W. Li, J. Stanojevic, T. Pohl *et al.*, Phys. Rev. Lett. **105**, 163201 (2010).
[38] This approach is expected to be valid for isolated *ns* Rydberg states considered here [24].
[39] K. Singer, J. Stanojevic, M. Weidemüller, and R. Côté, J. Phys. B **38**, S295 (2005).
[40] D. C. Roberts and S. Rica, Phys. Rev. Lett. **102**, 025301 (2009).
[41] O. N. Osychenko, G. E. Astrakharchik, F. Mazzanti, and J. Boronat, Phys. Rev. A **85**, 063604 (2012).